J|A|C|S
ARTICLES

Published on Web 10/02/2009

Anchoring of Rare-Earth-Based Single-Molecule Magnets on Single-Walled Carbon Nanotubes

Svetlana Kyatskaya,[†] José Ramón Galán Mascarós,[‡] Lapo Bogani,*[,§,||] Frank Hennrich,[†] Manfred Kappes,[†] Wolfgang Wernsdorfer,[§] and Mario Ruben*[,†]

Institut für Nanotechnologie, Karlsruhe Institute of Technology (KIT), D-76021 Karlsruhe, Germany, Institute of Chemical Research of Catalonia (ICIQ), Av. Països, Catalans 16, E-43007, Tarragona, Spain, 1. Physikalisches Institut, Universität Stuttgart, Pfaffenwaldring 57, D-70550, Stuttgart, Germany, and Institut Néel & Université J. Fourier, CNRS, Grenoble 25, Av. des Martyrs, F-38042, Grenoble, France

Received January 7, 2009; E-mail: lapo.bogani@pi1.physik.uni-stuttgart.de; mario.ruben@int.fzk.de

Abstract: A new heteroleptic bis(phthalocyaninato) terbium(III) complex **1**, bearing a pyrenyl group, exhibits temperature and frequency dependence of ac magnetic susceptibility, typical of single-molecule magnets. The complex was successfully attached to single-walled carbon nanotubes (SWNTs) using $\pi-\pi$ interactions, yielding a **1**−SWNT conjugate. The supramolecular grafting of **1** to SWNTs was proven qualitatively and quantitatively by high-resolution transmission electron microscopy, emission spectroscopy, and atomic force spectroscopy. Giving a clear magnetic fingerprint, the anisotropy energy barrier and the magnetic relaxation time of the **1**−SWNT conjugate are both increased in comparison with the pure crystalline compound **1**, likely due to the suppression of intermolecular interactions. The obtained results propose the **1**−SWNT conjugate as a promising constituent unit in magnetic single-molecule measurements using molecular spintronics devices.

Introduction

The development of new molecules and hybrid materials suited to single-molecule studies is a topic of considerable current interest. This is particularly true for the field of molecular spintronics, which holds great promise[1] but needs tailored magnetic molecules. One family of magnetic molecules that seems particularly promising is that of single-molecule magnets (SMMs), molecular complexes and clusters that display slow dynamics of the magnetization at low temperatures and an impressive array of quantum features. Combining SMMs with the domain of spintronics would not only allow exploiting these new properties but would also mean having unprecedented tools to study the fundamental processes governing magnetization dynamics.[1b] The field of molecular spintronics has thus received growing attention from the scientific community, and several approaches to its fundamental issues can be envisaged. One consists of immobilizing single magnetic molecules between two leads (or, respectively, between tip and surface) and then passing a current through the magnet. Although this approach has allowed the observation of several key issues, it has been impossible, up to now, to establish the magnetic bistability of individual SMMs, i.e., the hysteresis cycle opening at low temperatures. The lack of hysteresis might be due to the fact that the electrons passing through the molecule perturb the magnetization state of the molecules. In order to avoid the difficulties linked to the passage of electrons through the molecule, a different scheme has been envisaged, that of a so-called "spintronics double quantum dot".[1b] In this scheme, the SMM, which can be considered as a magnetic quantum dot, is weakly coupled to a molecular single-electron transistor, being the other molecular quantum dot. The magnetization of the molecule can then be read by its effect on the electron flow through the molecular quantum dot, with only weak perturbation of the SMM itself. Extensions of this concept include the recently developed nano-SQUID (superconducting quantum interference device),[2] whose high-sensitivity is due to the presence of a single-walled carbon nanotube (SWNT) in the loop. It is expected that such devices, as the SWNT cross-section is comparable to the dimensions of SMMs, will allow the detection of the single-molecule magnetic moments of a single molecule, an ambitious goal since Néel's pioneering work.[3] The switching of the magnetization of single molecules could also be detected using the nanomechanical properties of a suspended nanotube, which could act as a nanometer-sized vibrating sample magnetometer. The motion of the nanotube could be studied by the current through the nanotube itself. However, several challenges still remain to be solved before such spintronic schemes can be experimentally implemented. One is the fabrication of the double quantum dot device. While synthetic methods to graft nano-

[†] Karlsruhe Institute of Technology.
[‡] Institute of Chemical Research of Catalonia.
[§] Institut Néel & Université J. Fourier, CNRS.
[||] Universität Stuttgart.

(1) (a) Wolf, S. A.; Awschalom, D. D.; Buhrman, R. A.; Daughton, J. M.; von Molnár, S.; Roukes, M. L.; Chtchelkanova, A. Y.; Treger, D. M. *Science.* **2001**, *294*, 1488–1495. (b) Bogani, L.; Wernsdorfer, W. *Nat. Mater.* **2008**, *7*, 179–186. (c) Camarero, J.; Coronado, E. *J. Mater. Chem.* **2009**, *19*, 1678–1684. (d) Ferrer, J.; García-Suárez, V. M. *J. Mater. Chem.* **2009**, *19*, 1696–1717.

(2) Cleuziou, J.-P.; Wernsdorfer, W.; Bouchiat, V.; Ondarçuhu, T.; Monthioux, M. *Nat. Nanotechnol.* **2006**, *1*, 53–59.

(3) (a) Néel, L. *Ann. Geophys. (C.N.R.S.)* **1949**, *5*, 99–136. (b) Néel, L. C. R. *Proc. Natl. Acad. Sci. U.S.A.* **1949**, *228*, 664.

particles or photoactive molecules onto SWNTs have been developed in the last few years, only two reports have very recently appeared on grafting SMMs onto SWNTs,[4] and many questions remain open: What groups allow producing a sizable magnetic interaction without destroying the conductivity of the SWNTs? Are the magnetic properties retained when the grafting is performed? This last question is particularly important, as it has been shown that environmental effects are fundamental in SMMs and can lead to the progressive disappearance of the hysteresis when the steric or electronic influence of a substrate, e.g. of conducting surfaces, becomes considerable.[5] Only recently the persistence of SMM behavior in a monolayer of tetranuclear Fe(III) complexes bonded to a substrate[6] as well as Fe_6 wolframate molecules grafted on the side walls of SWNTs[4b] could be demonstrated. The second great challenge in the double quantum dot implementation is the characterization of the SMM behavior with the device. One of the great scientific challenges using these devices would be the possibility of probing a single, isolated molecule. However, as mentioned before,[5] environmental interaction and hybridization effects can exercise dramatic consequences on the magnetic properties, possibly yielding different results for SWNT−SMM or substrate−SMM conjugates than those observed for isolated SMMs in the highly homogeneous environment of a bulk 3D crystal. While tackling the challenge of single-molecule magnetism is certainly fascinating, the requirement for SMM conjugates eliminates an important reference point, posing a big experimental problem: in the conjugate device situation, how can one be sure that he/she is really probing the right molecule, i.e., respectively, the (magnetic) property of the molecule? A robust magnetic fingerprint for the molecule becomes an indispensable requirement for such cutting-edge experiments.

In this paper, we describe the creation and magnetic characterization of a hybrid conjugate composed of SWNTs and a Tb(III)-based single metal ion SMM, which constitutes a solution to some of these problems. The SMM behavior of mononuclear rare-earth (M) complexes in a low symmetry environment was first reported by Ishikawa and co-workers[7−9] on bis(phthalocyaninato) complexes $[Pc_2M]^{-/0/+}$ (Pc = anion of phthalocyanine) of Tb(III), Dy(III), and Ho(III).

This class of complexes shows large magnetic anisotropies and slow relaxation of the magnetization in a temperature range significantly higher than that of all other known SMMs.[10−14] Moreover, Kramer's theorem of spin parity provides a fingerprint of the magnetic behavior of these systems. The theorem states that no matter how asymmetric the crystal field is, a system possessing an odd number of electrons must have a ground state that is at least doubly degenerate, even in presence of crystal field or spin−orbit interactions. This means that no avoided level crossing, and thus no zero field quantum tunnelling, can be present for half-integer spins. In the case of rare-earths, due to strong hyperfine interactions, the electronic spin number J is not a good quantum number to calculate parity effects and the sum of nuclear and electronic spin numbers is more appropriate. The quantum tunnelling of the magnetization, in particular, shows zero-field tunnelling only for rare-earths whose summed electronic and nuclear moments give an integer spin. Such effects are extremely robust, as they depend on the intrinsic symmetry of the environment, and not on possible ligand field distortions or electronic perturbations. They constitute a perfect example of the desired fingerprint of the magnetic behavior. The case of Tb(III) is of particular interest, as hyperfine and nuclear quadrupole interactions need to be considered to explain the magnetic behavior of $[Pc_2Tb]^{-/0/+}$ compounds. Also for the terbium complexes, the out-of-phase component of the dynamic magnetic susceptibility appears well above 40 K, due to an unusually high-energy barrier for reversal of the magnetization, ΔE. ΔE can be increased even further by oxidizing the ligand from the anion[7,9,14] $[Pc_2Tb]^-$ to the neutral form[8] $[Pc_2Tb]^0$ and even further on to the cation[15] $[Pc_2Tb]^+$.

Such striking magnetic properties are coupled to a very robust single metal ion structure, which is expected to retain its magnetic properties in different environmental conditions, unlike that of many of the structurally more complex d-metal SMMs.[10−13] Thus, the electronic structure of isolated bis(phthalocyaninato) terbium(III) molecules, supported on the Cu(111) surface, has been characterized by density functional theory and scanning tunneling spectroscopy. These studies reveal that the interaction with the metal surface preserves both the molecular structure and the large spin magnetic moment of the metal center on metallic surfaces.[16] Furthermore, Kondo-physics behavior was reported for molecules deposited on a Au(111) surface, giving evidence for retained magnetic behavior.[17]

So far the unsubstituted complexes $[Pc_2Tb]^0$ afford no molecular ordering on pyrolitic graphite or metallic surfaces

(4) (a) Bogani, L.; Danieli, C.; Biavardi, E.; Bendiab, N.; Barra, A.-L.; Dalcanale, E.; Wernsdorfer, W.; Cornia, A. *Angew. Chem., Int. Ed.* **2009**, *48*, 746–750. (b) Giusti, A.; Charron, G.; Mazerat, S.; Compain, J.-D.; Mialane, P.; Dolbecq, A.; Rivière, E.; Wernsdorfer, W.; Biboum, R. N.; Kieta, B.; Nadjo, L.; Filoramo, A.; Bourgoin, J.-P.; Mallah, T. *Angew. Chem., Int. Ed.* **2009**, *48*, 4949–4952.
(5) (a) Bogani, L.; Cavigli, L.; Gurioli, M.; Novak, R. L.; Mannini, M.; Caneschi, A.; Pineider, F.; Sessoli, R.; Clemente-León, M.; Coronado, E.; Cornia, A.; Gatteschi, D. *Adv. Mater.* **2007**, *19*, 3906–3911. (b) Mannini, M.; Sainctavit, P.; Sessoli, R.; Moulin, C. C. D.; Pineider, F.; Arrio, M. A.; Cornia, A.; Matteschi, D. *Chem.−Eur. J.* **2008**, *14*, 7530–7435.
(6) Mannini, M.; Pineider, F.; Sainctavit, P.; Danieli, C.; Otero, E.; Sciancalepore, C.; Talarico, A. M.; Arrio, M.-A.; Cornia, A.; Gatteschi, D.; Sessoli, R. *Nat. Mater.* **2009**, *8*, 194–197.
(7) (a) Ishikawa, N.; Sugita, M.; Ishikawa, T.; Koshihara, S.; Kaizu, Y. *J. Am. Chem. Soc.* **2003**, *125*, 8694–8695. (b) Ishikawa, N.; Sugita, M.; Wernsdorfer, W. *J. Am. Chem. Soc.* **2005**, *127*, 3650–3651. (c) Ishikawa, N.; Sugita, M.; Ishikawa, T.; Koshihara, S.; Kaizu, Y. *J. Phys. Chem. B* **2004**, *108*, 11265–11271.
(8) Ishikawa, N.; Sugita, M.; Tanaka, N.; Ishikawa, T.; Koshihara, S.; Kaizu, Y. *Inorg. Chem.* **2004**, *43*, 5498–5500.
(9) Ishikawa, N.; Sugita, M.; Wernsdorfer, W. *Angew. Chem., Int. Ed.* **2005**, *44*, 2931–2935.
(10) Gatteschi, D.; Sessoli, R.; Villain, J. *Molecular Nanomagnets*; Oxford University Press: New York, 2006.
(11) Sessoli, R.; Tsai, H.-L.; Schake, A. R.; Wang, S.; Vincent, J. B.; Folting, K.; Gatteschi, D.; Christou, G.; Hendrickson, D. N. *J. Am. Chem. Soc.* **1993**, *115*, 1804–1816.
(12) Zheng, Y.-Z.; Lan, Y.; Anson, C. E.; Powell, A. K. *Inorg. Chem.* **2008**, *47*, 10813–10815.
(13) Cangussu, D.; Pardo, E.; Dul, M.-C.; Lescouzec, R.; Herson, P.; Journaux, Y.; Pedroso, E. F.; Pereira, C. L. M.; Stumpf, H. O.; Muòoz, M. C.; Ruiz-García, R.; Cano, J.; Julve, M.; Lloret, F. *Inorg. Chim. Acta* **2008**, *361*, 3394–3402.
(14) (a) Ishikawa, N.; Sugita, M.; Okubo, T.; Tanaka, N.; Lino, T.; Kaizu, Y. *Inorg. Chem.* **2003**, *42*, 2440–2446. (b) Branzoli, F.; Carretta, P.; Filibian, M.; Zoppellaro, G.; Graf, M. J.; Galán-Mascarós, J. R.; Fuhr, O.; Brink, S.; Ruben, M. *J. Am. Chem. Soc.* **2009**, *131*, 4387–4396.
(15) Takamatsu, S.; Ishikawa, T.; Koshihara, S.; Ishikawa, N. *Inorg. Chem.* **2007**, *46*, 7250–7252.
(16) Vitali, L.; Fabris, S.; Mosca Conte, A.; Brink, S.; Ruben, M.; Baroni, S.; Kern, K. *Nano Lett.* **2008**, *8*, 3364–3368.
(17) Katoh, K.; Yoshida, Y.; Yamashita, M.; Miyasaka, H.; Breedlove, B. K.; Kajiwara, T.; Takaishi, S.; Ishikawa, N.; Isshiki, H.; Zhang, Y. F.; Komeda, T.; Yamagishi, M.; Takeya, J. *J. Am. Chem. Soc.* **2009**, *131*, 9967–9976.

but only the instantaneous formation of molecular aggregates.[18] Thus, a chemical engineering of the complex is necessary to obtain hybrid SWNT−SMM materials. The rich and well-studied chemistry of phthalocyanines allows adding tailored functionalities to these SMMs, so as to organize them in hybrid structures[18] while the SMM behavior is maintained. Thus, $[Pc_2Tb]^{-/0/+}$ family constitutes a very interesting class of compounds that possess optimal characteristics for grafting onto SWNTs.

Here we report the synthesis of a new pyrenyl-substituted heteroleptical bis(phthalocyaninato)Tb(III) SMM (**1**), which constitutes an appealing candidate for SMM−SWNT hybrids. We demonstrate that this molecule can be subsequently confined on to sidewalls of SWNTs under the persistence of pivotal magnetic properties, some characteristics even being improved. Among the chemical approaches for the grafting of organic molecules to SWNTs, we have chosen the functionalization by a noncovalent interaction via pyrene linkers to avoid possible insertion of local defects by covalent bonding that may disrupt the SWNT conducting properties.[19−21] Moreover, recently, successful grafting of a compound of the Fe_4 SMM family containing a pyrene moiety on to CNTs has been reported.[4a]

Experimental Section

General Synthetic Remarks. Reactions requiring an inert gas atmosphere were conducted under argon, and the glassware was oven-dried (140 °C). All reagents were purchased from commercial sources and used as received. Radial chromatography was performed on Chromatotron 7924T, with plates prepared from Silica gel $60PF_{254}$ containing gypsum. $PcLi_2$ (**4**),[22] 1,2-dicyano-4,5-dihexylbenzene (**7**),[23] and 1-pyrenebutanol (**12**)[24] were prepared according to the literature procedures.

Synthesis of 1-Bromobutylpyrene (13). 1-Bromobutylpyrene was obtained by a variation of the reported procedure.[25] To a solution of 1-pyrenebutanol **12** (2.32 g, 8.5 mmol) in dry benzene (50 mL) phosphorus tribromide (1.16 g, 4.3 mmol) was slowly added at 5 °C (ice bath). After the addition was complete, the reaction was kept at room temperature until the starting compound **12** disappeared (ca. 1.5 h, TLC control). The mixture was poured into ice−water (200 mL) and then extracted with diethyl ether (3 × 100 mL). The combined organic layers were washed twice with water and dried over magnesium sulfate. The solvent was removed under reduced pressure, and the residue was chromatographed on SiO_2 to give 1-bromobutylpyrene **13** (1.3 g, 45% yield), which was recrystallized from light petroleum. Mp: 85−89 °C. ^{1}H NMR (CD_2Cl_2; δ, ppm): 1.97−2.05 (m, 4 H), 3.34−3.39 (m, 2 H), 3.45−3.50 (m, 2 H), 7.87 (d, J = 9 Hz, 1 H), 7.96−8.03 (m, 3 H); 8.06−8.11 (m, 4H), 8.14 (d, J = 9 Hz, 1 H). ^{13}C NMR ($CDCl_3$; δ, ppm): 30.23, 32.62, 32.65, 33.66, 123.26, 124.78, 124.84, 124.96, 125.02, 125.12, 125.87, 126.71, 127.23, 127.38,127.51, 128.62, 129.92, 130.90, 131.43, 136.08. MALDI-ToF calcd for $C_{20}H_{17}Br$: 336.0508. Found: 335.7416.

Synthesis of the Asymmetrically Substituted Phthalocyanine A_3B (9). Lithium metal (35 mg, 5.04 mmol) was dissolved in 1-pentanol (25 mL) at 80 °C under an atmosphere of dry N_2. To this lithium pentanolate solution were added **7** (1.15 g, 3.88 mmol) and **8** (0.13 g, 0.32 mmol), and the reaction mixture was heated at 135 °C for 3 h. On cooling, the dark blue-green solution was treated with glacial acetic acid (25 mL). The resultant precipitate was collected by filtration; washed thoroughly with water, methanol, and Et_2O; and then dried on air to yield a mixture (by MALDI-ToF, main components, A_3B, A_4; minor components, A_2B_2, AB_3, B_4) as a dark blue-green powder (630 mg). The product mixture was dissolved in a minimum amount of chloroform, and the solution was subjected to column chromatography (SiO_2), eluting with $CHCl_3$. The first fraction was collected. After removal of the solvent under reduced pressure, the blue residue was dried at 50 °C to afford 0.34 g (47%) of **10** (R_f = 0.78; chloroform/hexane, 5/3 vv). The second fraction (representing a mixture of two compounds with R_f = 0.78 and 0.25) was initially applied to a radial chromatograph eluting with chloroform/hexane (5/3 vv) to remove a trace amount of A_4 and then separated with chloroform to afford after removal of the solvent under reduced pressure and desiccation at 50 °C a green powder, phthalocyanine **9** (98 mg, 24%, R_f = 0.25; chloroform/hexane, 5/3 vv).

A_3B (9). ^{1}H NMR ($CDCl_3$; δ, ppm): 0.89−1.12 (m, 20 H), 1.32 (s, 12 H,), 1.53−2.34 (m, 54 H), 3.61 (m, 2 H), 7.57−8.39 (m, 17 H); 8.45 (d, J = 9 Hz, 1 H). MALDI-ToF calcd for $C_{88}H_{106}N_8O$: 1291.8516. Found: 1290.0271.

A_4 (10). ^{1}H NMR ($CDCl_3$; δ, ppm): 0.87−1.12 (m, 24 H), 1.32 (s, 16 H,), 1.53−2.34 (m, 64 H), 3.31 (br. s, 2 H−N), 8.65 (br s, 8 H). MALDI-ToF calcd for $C_{80}H_{112}N_8$: 1184.9004. Found: 1183.9338.

Synthesis of 4-(4-Pyren-1-ylbutoxy)phthalonitrile (8). 8 was obtained according to the reported procedure[26] with some modification. A mixture of 1-bromobutylpyrene (**13**) (1.07 g, 3.2 mmol), 4-hydroxyphthalonitrile (**14**) (0.57 g, 3.9 mmol), and K_2CO_3 (2.09 g) in the mixture of DMSO and acetone (15 mL, 15 mL) in two-necked round-bottom flask was heated at 60 °C overnight until the starting compound **13** disappeared (TLC control). The reaction mixture was poured into 200 mL of ice−water, and the precipitate formed was collected by filtration and washed with water until pH 7 and than with methanol and ether. Crude product was recrystallized from acetone/1,4-dioxane mixture to afford 1.15 g (77%) of **8** as yellowish powder. Mp: 154−157 °C. ^{1}H NMR ($CDCl_3$; δ, ppm): 1.95−2.105 (m, 4 H), 3.42 (t, J = 8 Hz, 2 H), 3.92 (t, J = 6 Hz, 2 H), 6.93 (dd, ^1J = 9 Hz, ^2J = 2 Hz, 1 H), 7.05 (d, J = 2 Hz, 1 H); 7.47 (d, J = 9 Hz, 1 H), 7.85 (d, J = 8 Hz, 1H), 7.97 (d, J = 7 Hz, 1 H), 8.01 (br s, 2 H), 8.06−8.10 (m, 2 H), 8.14−8.17 (m, 2 H), 8.22 (d, J = 8 Hz). ^{13}C NMR ($CDCl_3$; δ, ppm): 27.83, 29.00, 33.50, 69.19, 107.33, 117.57, 119.45, 119.64, 123.54, 125.17, 125.23, 125.54, 125.29, 126.41, 127.24, 127.69, 127.77, 127.84, 128.97, 130.37, 131.17, 131.78, 135.30, 136.24, 162.22. MALDI-ToF calcd for $C_{28}H_{20}N_2O$: 400.1570. Found: 399.8239.

Synthesis of Lithium Phthalocyanine [A_3B−Li_2] (2). Under an argon atmosphere, 85.7 mg (0.066 mmol) of phthalocyanine A_3B (**9**) was added to a solution of Li (0.12 mg, 0.016 mmol) in ethyl alcohol (10 mL). A green color appeared, and when the mixture was warmed, the color changing to deep blue. The mixture was refluxed for 2 h and cooled, the solvent was removed under reduced pressure, and the residue of dull blue lithium phthalocyanine was extracted with acetone, previously dried over sodium sulfate, to remove basic lithium compounds. Evaporation under reduced pressure and desiccation under an argon atmosphere left dilithium phthalocyanine **2** as a crystalline purple powder (yield, 67 mg;

(18) (a) Gómez-Segura, J.; Díez-Pérez, I.; Ishikawa, N.; Nakano, M.; Veciana, J.; Ruiz-Molina, D. *Chem. Commun.* **2006**, 2866–2868. (b) Ye, T.; Takami, T.; Wang, R.; Jiang, J.; Weiss, P. S. *J. Am. Chem. Soc.* **2006**, *128*, 10984–10985. (c) Su, W.; Jiang, J.; Xiao, K.; Chen, Y.; Zhao, Q.; Yu, G.; Liu, Y. *Langmuir* **2005**, *21*, 6527–6531.
(19) Bogani, L.; Wernsdorfer, W. *Nat. Mater.* **2008**, *7*, 179–186.
(20) Bogani, L.; Wernsdorfer, W. *Inorg. Chim. Acta* **2008**, *361*, 3807–3819.
(21) Gãmez-Navarro, C.; De Pablo, P. J.; Gãmez-Herrero, J.; Biel, B.; Garcia-Vidal, F. J.; Rubio, A.; Flores, F. *Nat. Mater.* **2005**, *4*, 534–539.
(22) Barrett, P. A.; Frye, D. A.; Linstead, R. P. *J. Chem. Soc.* **1938**, 1157–1163.
(23) Hanack, M.; Haisch, P.; Lehmann, H.; Subramanian, L. R. *Synthesis* **1993**, *4*, 387–390.
(24) Yamana, K.; Letsinger, R. L. *Nucleic Acids Symp. Ser.* **1985**, *169*, 72.
(25) Leardini, R.; Nanni, D.; Peduli, G.; Tundo, A.; Zanardi, G.; Foresti, E.; Palmieri, P. *J. Am. Chem. Soc.* **1989**, *111*, 7723–7739.
(26) Mutsumi, K.; Takahisa, K.; Kazuchika, O.; Kenji, H.; Hirofusa, S.; Nagao, K. *Langmuir* **2003**, *19*, 4825–4830.

78%). The compound is unstable and has to be used for the next step during the next few days. ^{1}H NMR (acetone-d_6; δ, ppm): 0.89−1.12 (m, 20 H), 1.32 (s, 12 H), 1.53−1.74 (m, 54 H), 3.21 (br s, 8 H), 4.63 (br s, 2 H), 7.58 (br s, 1 H), 8.0−8.31 (m, 17 H), 8.59 (d, J = 9 Hz, 1 H), 9,14 (br s, 8 H). MALDI-ToF calcd for $C_{88}H_{104}N_8OLi_2$: 1301.7491. Found: 1302.8651.

Synthesis of the Heteroleptic Bis(phthalocyaninato)terbium(III) Complex (1). Under a slow stream of Ar, a mixture of $PcLi_2$ (**4**) (68 mg, 0.13 mmol) and $Tb(acac)_3 \cdot 2H_2O$ (**5**) (59 mg, 0.13 mmol) in 1-chloronaphtalene (5 mL), percolated through a basic alumina column just before being used, was heated at 185−195 °C for 1 h until free **4** was no longer detected. The resulting dark blue solution was cooled down and **2** (160 mg, 0.11 mmol) was added. The mixture was heated up to 200−210 °C for 1 h until free **2** was no longer detected (MALDI-ToF control). The mixture was subjected to column chromatography (basic alumina oxide, 60 g), eluting with CH_2Cl_2/hexane (7/4 vv). 1-Chloronaphtalene was eluted first and then a greenish-blue band was collected and concentrated to yield a product mixture (by MALDI-TOF, main components are $[A_3B-TbPc]^{0/-}$, $(A_3B)Pc_2Tb_2]$ and minor components are $[A_3B-Tb-A_3B]^{0/-}$, $[PcTbPc]^{0/-}$) as a dark blue-green powder (150 mg). The complex **1** was separated from the crude mixture by column chromatography (basic alumina oxide), eluting with CH_2Cl_2/MeOH (10:1) followed by reprecipitation from the hexane/CH_2Cl_2 mixture to afford a deep green solid of neutral **1** (87 mg, 24% yield from **2**; R_f = 0.38; CH_2Cl_2). MALDI-ToF calculated for $C_{120}H_{120}N_{16}OTb$ (M^+): 1960.9110. Found 1959.3799 (M^+, 100%).

The symmetrical complex **6** with two pyrene anchors was achieved by eluting with CH_2Cl_2/MeOH (2:1) mixture as a green compound (9 mg, R_f = 0.56; CH_2Cl_2/MeOH (10:3)). MALDI-ToF calcd for $C_{176}H_{208}N_{16}O_2Tb$ (M^+): 2735.1264. Found 2736.9281 (M^+, 100%).

Purification of Carbon Nanotubes. Typically, 10 mg of SWNT material (HiPco, Unidym) was suspended in 25 mL of H_2O with 1 wt % of SCholate using a tip sonicator (Bandelin, 200 W maximum power, 20 kHz, in pulsed mode with 100 ms pulses) applied for 2 h at ∼20% power. A density gradient centrifugation (DGC)[27] step was then used to remove larger agglomerates, amorphous carbon, and catalyst particles while retaining SWNTs. However, rather than preformed gradients, we used self-generated gradients of Iodixanol plus 1 wt % of SCholate. Ultracentrifugation (Optima Max-E, Beckman-Coulter) was carried out in a fixed-angle rotor (ML-80, Beckman-Coulter) at 15 °C and at 45 000 rpm for 18−20 h using a polyallomer (8 mL Bell top Quick-Seal, Beckmann-Coulter) centrifuge tubes. This rotation speed results in centripetal accelerations of 103 650g and 140 400g, at the average/maximal radii of 45.7/61.9 mm, respectively. After centrifugation, different colored regions—approximately 5 mL of the whole 8 mL from bottom to top—are visible. Of these, only the last (i.e., topmost) ∼0.5 mL contains pure SWNTs. This last fraction was then isolated and used as the starting suspension for gel filtration.

Gel filtration was performed using Sephacryl S-500 gel filtration medium (Amersham Biosciences) in a glass column of 20 cm length and 2 cm inner diameter. After filling the glass column with the filtration medium, the gel was slightly compressed to yield a final height of 14 cm. For the separation, 10 mL of SWNT starting suspension was applied to the top of the column and a solution of 1 wt % SCholate in H_2O as eluant was pushed through the column by applying sufficient pressure with compressed air to ensure a flow of ∼1 mL/min. Fractions were collected in 3−4 mL portions. After applying ∼50 mL, most of the SWNTs (consisting of mainly individualized SWNTs in a ca. 2:1 mixture of metallic and semiconducting ones) were eluted, whereas smaller particles (residue amorphous carbon and metal particles) remain on the column. In order to prove the magnetic purity of the purified SWNTs, we checked them before the grafting of the SMMs. Since even after the first purification cycle a small quantity of catalyst could still be detected, the gel filtration was performed twice. No out-of-phase-signal in magnetic susceptibility measurements could be detected after the second purification cycle.

Preparation of the 1−SWNT Hybrids. The SWNT−SCholate suspension was diluted with acetone, and the SWNTs were collected by filtration and washed extensively with water to remove the cholate and then dried. The obtained SWNTs (2.5 mg) were redispersed in a solution of 3.3 mg of **1** in 5 mL of dry and argon-saturated CH_2Cl_2, and the reaction mixture was stirred for 48 h; whereupon, the green color of supernatant disappeared. The resulting mixture was sonicated for 6 h at 20 °C followed by centrifugation for 2 h. The precipitate was collected by centrifugation, washed several times with CH_2Cl_2, and desiccated under a slow stream of argon. A 4.9 mg portion of the hybrid material was used for ac susceptibility measurements.

Spectroscopic Characterization. UV/visible/NIR spectra were measured on a Varian Cary 500 Scan UV/vis/NIR spectrophotometer by using a 1 cm optical path length quartz cell. Fluorescence spectra were measured on a Varian Cary Eclipse Fluorescence spectrophotometer by using a 1 cm optical path length quartz cell. MALDI-ToF spectra were recorded on a Perseptive Biosystems Voyager-DePro. NMR spectra were recorded at room temperature on a Bruker 300 Ultrashield series instrument. Melting points were measured with Büchi B-545 using open-ended glass capillaries.

Electrochemistry. The cyclic voltammogram was recorded on an EG&G Model 263A potentiostat using a three-electrode system in solvents containing 0.1 M n-Bu_4NClO_4 as the supporting electrolyte. A platinum button electrode was used as the working electrode. A platinum wire served as the counter electrode, and Ag/AgCl was used as the reference electrode. The ferrocene/ferrocenium (Fc/Fc+) redox couple was used as an internal standard.

Microscopies. TEM specimens were prepared by dropping a suspension of the **1**−SWNT conjugate from dry dichloromethane onto carbon-coated copper grids (Plano GMbH, 200 mesh). The TEM investigations were performed on a FEI Tecnai F20 ST microscope operated at an accelerating voltage of 200 kV. AFM images were acquired using a Veeco Nanoman D3100 instrument in tapping mode.

Magnetic Measurements. The ac and dc magnetic susceptibility measurements were carried out on a SQUID magnetometer by Quantum Design, model MPMS-XL-5. Hysteresis cycles were acquired with a homemade micro-SQUID setup.[28]

Results and Discussion

Synthesis. The heteroleptic bis(phthalocyaninato)terbium(III) complex **1** was synthesized by a multistep convergent method (Scheme 1).[29] Two different phthalocyaninato lithium salts (**2** and **4**) and $[Tb(acac)_3 \cdot 2H_2O]$ (acac = acetylacetonato) (**5**) were reacted in a 1:1:1 ratio under reflux in 1-chloronaphhalene leading to a mixture of mono- and binuclear complexes, whose formation was monitored during the course of the reaction by thin-layer chromatography and matrix-assisted laser desorption/ionization-time-of-flight mass spectrometry (MALDI-ToF MS). The isolation of the neutral target complex $[A_3B-Tb^{III}Pc]^0$ (**1**) was achieved via column chromatography on basic alumina oxide followed by reprecipitation from a CH_2Cl_2−hexane mixture.

The unsymmetrical monophtalocyanine ligand **9** was synthesized by statistical condensation of a 10:1 molar ratio of **7** (A moiety) and **8** (B moiety) in lithium pentanolate solution

(27) Arnold, M. S.; Green, A. A.; Hulvat, J. F.; Stupp, S. I.; Hersam, M. C. *Nat. Nanotechnol.* **2006**, *1*, 60–65.

(28) Wernsdorfer, W.; Hasselbach, K.; Mailly, D.; Barbara, B.; Thomas, L.; Suran, S. *J. Magn. Magn. Mater.* **1995**, *145*, 33–39. (b) Wernsdorfer, W. *Supercond. Sci. Technol.* **2009**, *22*, 064013/1–064013/13.

(29) Pondaven, A.; Cozien, Y.; L'Her, M. *New J. Chem.* **1992**, *16*, 711–718.

Scheme 1. Schematic Representation of the Synthesis of **1**

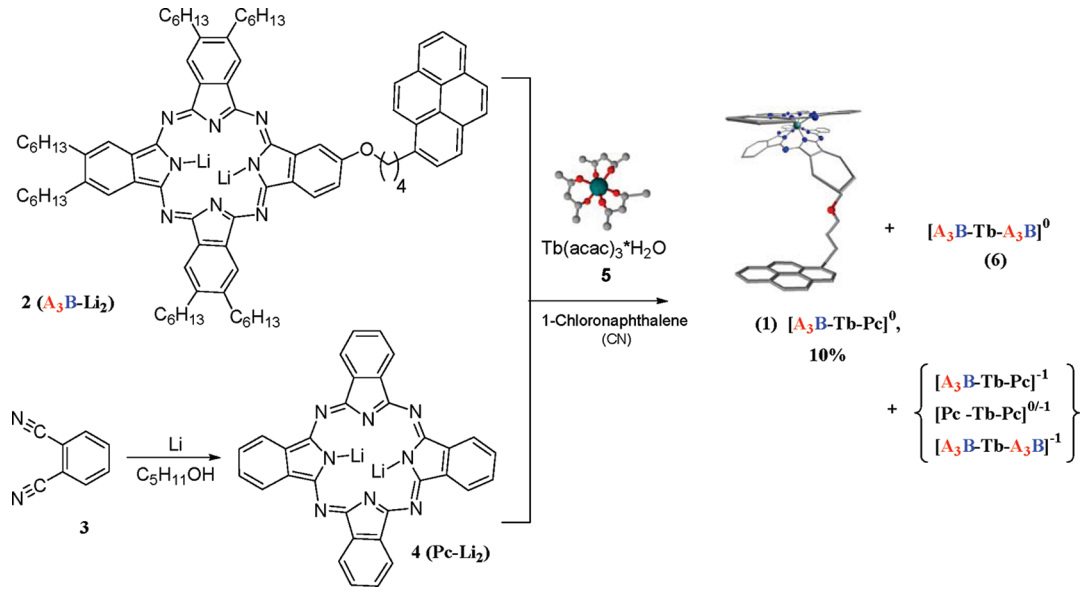

Scheme 2. Schematic Representation of the Synthesis of **2**

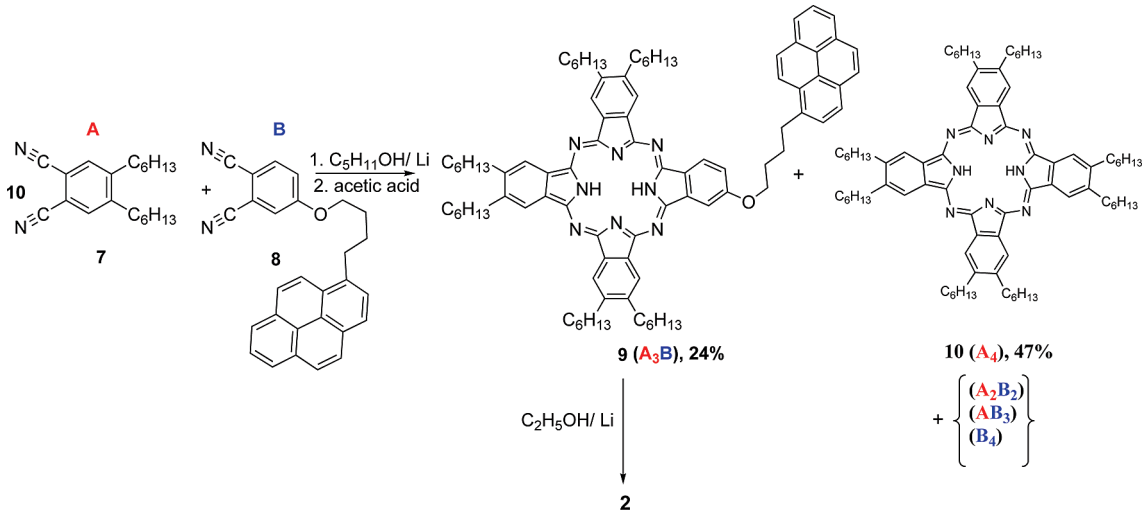

under reflux for 3 h, as shown in Scheme 2. The resulting products contain a mixture of several possible topoisomeres, i.e. a total of five species with different masses. MALDI-ToF MS investigation of the mixture reveals that A_3B and A_4 constitute the main components (24% and 47%, respectively), while A_2B_2, AB_3, and B_4 are minor components. Monophtalocyanines with identical (A_4) or different substituents (A_3B) can then be isolated from this mixture via radial chromatography on silica gel, thus leading to the desired phtalocyanine to be used to create the heteroleptic bis-phthalocyaninato compound.

The B moiety, 4-(4-pyren-1-ylbutoxy)phthalonitrile (**8**), was synthesized as shown in Scheme 3. Reduction of 4-pyren-1-ylbutyric acid (**11**) gives 4-(1-pyrenyl)butanol (**12**), which is then converted into 1-bromobutylpyrene (**13**) in presence of phosphorus tribromide. Subsequent coupling with 4-hydroxy-phthalonitrile (**14**) in a mixture of DMSO and acetone in the presence of K_2CO_3 gives **8** in a good yield (77%).

Structural Characterization of 1. Complexes **1** and **6**, due to the presence of delocalized unpaired electrons, are NMR silent. Conclusive ^{1}H NMR investigations could be acquired for the respective anionic forms, obtained in $CDCl_3$ after the reduction by hydrazine hydrate. The ^{1}H NMR spectrum of the $[A_3B-Tb^{III}Pc]^-$ anion shows manifold, broad, superimposed multiplets of the ring protons (Pc and A_3B) together with signals assignable to the protons in the side chains and in the pyrene group. All bands show strong paramagnetic upfield shifts, with the farthest band at $\delta = -63$ ppm, while the homoleptic parent complex $[Pc_2Tb]^-$ exhibits in solution only two signals with dipolar shifts for α-protons ($\delta = -82.38$ ppm) and β-protons ($\delta = -39.10$ ppm) of the phthalocyanine ligands.[14]

High-resolution MALDI-ToF MS spectra of compounds **1**, **2**, **4**, **6**, and **9** (see Figures 3S, 7S, and 8S in the Supporting Information) prove the heteroleptic nature of **1** bearing two different types of macrocycles (Pc and A_3B). For all compounds, intense ionic signals, corresponding to the intact singly charged molecular ions, were observed. In all cases, the molecular ion was the most abundant high mass ion with distinct isotopic distributions. The relative abundances of the isotopic ions are in good agreement with the simulated spectra, as reported in Table 1S (Supporting Information), where the mass spectral results and calculated values are summarized.

Scheme 3. Synthesis of 4-(4-Pyren-1ylbutoxy)phthalonitrile (**8**)

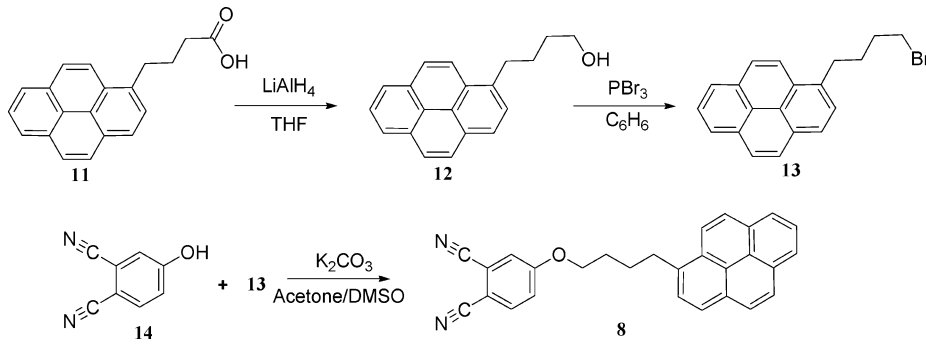

The electrochemical behavior of a $[Pc_2Lu]^0$ complex has been reported exhibiting two reversible redox waves at 0.0 and −0.4 V.[30] It was shown that the incorporation of electron-donating groups into the Pc-macrocycle of $[Pc'_2Ln]^0$ complexes (Ln = Eu, Gd, Yb, Lu) renders the respective Pc′-ligands more difficult to reduce in comparison with the unsubstituted complexes.[30] The electrochemical behavior of complex **1** was studied by cyclic voltammetry (CV) obtained at Pt electrode from a solution of **1** in methylene chloride containing 0.1 M $[n\text{-}Bu_4N][ClO_4]$ (Figure 10S, Supporting Information). Two quasireversible monoelectronic redox systems appear near −0.19 and −0.61 V, due to the reduction of the pthtalocyanine ligands and in accordance with the electron-donating nature of the substituents. In addition, the cyclic voltammogram of **1** exhibits an irreversible oxidation at 0.64 V attributed to the oxidative coupling of the pyrene moiety as the reported literature value.[31]

Assembly of the Hybrid 1−SWNT Conjugate. The pyrenyl group is known to interact strongly with SWNTs via π-stacking interactions. This has been used, for example, in the production of SWNT−nanoparticle hybrids,[4a] the grafting of proteins and other biological molecules to SWNTs,[32] and to immobilize light-harvesting groups on the SWNT, as well as in the design of new photoelectric devices.[33] Following this strategy, the SWNTs were strongly purified by ultracentrifugation and gel filtration to remove all magnetic iron catalyst particles. The so gained SWNTs were proven to be diamagnetic in magnetic susceptibility measurements and did not show any out-of-phase-signal in ac measurements. A sample of highly purified SWNTs (1 mg) was dispersed by overnight sonication in a solution of **1** (5 mg) in dry dichloromethane (25 mL) saturated with nitrogen.

Transmission electron microscopy (TEM) inspection of pristine SWNTs did not reveal any externally grafted objects, as shown in Figure 1a. In contrast, the TEM images after treatment with **1** show isolated SWNTs where fixed molecules of **1** can be clearly distinguished as darker marks. Inspection of the TEM images indicates that the grafted objects possess a diameter of about 1 nm, in accordance with the size of complex **1**. The energy-dispersive X-ray (EDX) spectroscopy study proves the presence of terbium in the area of the grafted objects (Figure 1c).

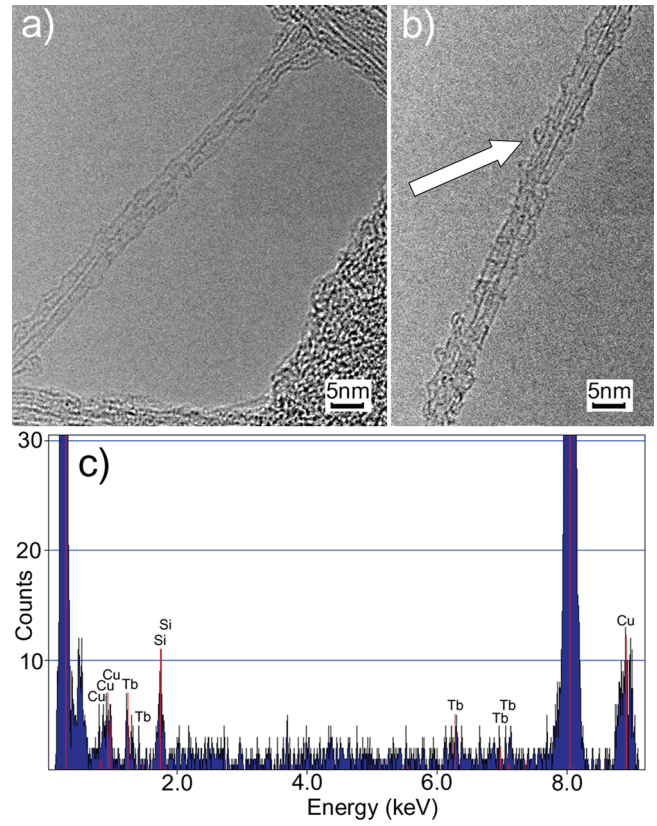

Figure 1. HR-TEM image of (a) a bundle of two pristine SWNTs, (b) a bundle of two SWNTs decorated with complex **1**, and (c) the EDX spectrum of the **1**−SWNT conjugate taken from the area depicted in part b. The blue curve corresponds to the experimental spectrum; the red lines show the energy of the bands.

Atomic force microscopy (AFM) experiments were carried out to characterize the **1**−SWNT conjugate further. AFM height images performed in tapping mode show the appearance of protrusions on the SWNTs (Figure 2a), whereby only few molecules are grafted on the SWNT surface. Statistical inspection of the heights of the spots reveals a rather narrow distribution of sizes (Figure 2b), indicating a mean height of 1 nm, compatible with the dimensions of **1**. The lateral AFM resolution does not allow a quantitative estimation of the number of grafted SMMs, as the size of the complex **1** is comparable to that of SWNTs, which precludes exact lateral differentiation.

(30) (a) L'Her, M.; Cozien, Y.; Courtot-Coupez, J. *J. Electroanal. Chem.* **1983**, *157*, 183–187. (b) Markovitsi, D.; Tran-Thi, T.-H.; Even, R.; Simon, J. *Chem. Phys. Lett.* **1987**, *137*, 107–112. (c) Pondaven, A.; Cozien, Y.; L'Her, M. *New J. Chem.* **1991**, *15*, 515–516. (d) Jiang, J.; Liu, R. C. W.; Mak, T. C. W.; Chan, T. W.D.; Ng, D. K. P. *Polyhedron* **1997**, *16*, 515–520.
(31) (a) Coleman, A.; Pryce, M. T. *Inorg. Chem.* **2008**, *47*, 10980–10990. (b) Lu, G.; Shi, G. *J. Electroanal. Chem.* **2006**, *586*, 154–160.
(32) Chen, R. J.; Zhang, Y.; Wang, D.; Dai, H. *J. Am. Chem. Soc.* **2001**, *123*, 3838–3839.
(33) D'Souza, F.; Chitta, R.; Sandanayaka, A. S. D.; Subbaiyan, N. K.; D'Souza, L.; Araki, Y.; Ito, O. *J. Am. Chem. Soc.* **2007**, *129*, 15865–15871.

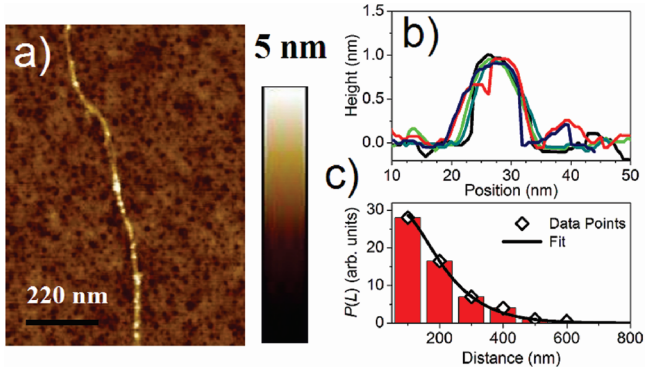

Figure 2. (a) AFM topography of the **1**−SWNT conjugate on a SiO_2 surface. (b) Analysis of the AFM heights of the grafted molecules, showing the highly monodisperse size around 1 nm. The width of the spots corresponds to the width of the AFM tip used. (c) Statistical distribution of distances between spots on a SWNT and fit to the data (see the text).

The distribution of distances between randomly placed objects along a line has a characteristic statistical shape,[34] given by the form: $P(L) = L \exp(-CL)$, where $P(L)$ is the probability of finding a segment of length L and C is the linear concentration of objects on the line. Similar expressions have been used to calculate the statistical distance between two defects in a genomic sequence[35] or to determine the ensemble of magnetic segments in doped magnetic chains.[36] As $P(L)$ depends on C the statistical analysis of the distances between the detectable molecules can give an indication of the number of SMMs on the SWNTs (Figure 2c). This method is more reliable than just counting the number of protrusions on the SWNT, because it allows extrapolating, on the assumption that the objects are randomly placed, those complexes of **1** that lie too close to one another to be detectable by AFM and thus appear as a single spot in the image. The curve obtained is reported in Figure 2c, together with a fit to the expected expression ($R^2 = 0.998$), which affords $C = 12.5$ molecules per micrometer. This means that the number of detectable molecules on the SWNTs is about 1 for every 80 nm of SWNT length. Supposing that about three-fourths of the complexes of **1** stick in fact besides the SWNT, as observed before for a different SMMs,[4] a linear concentration of one molecule for every 11 nm of SWNT can be obtained, in overall agreement with the value extracted with atomic emission spectroscopy (vide infra).

Quantitative investigation of the Tb content in the **1**−SWNT conjugate was carried out with inductively coupled plasma atomic emission spectroscopy, revealing a Tb mass percentage of 4.57%; corresponding to one Tb atom every 300 C atoms. Considering that SWNTs of about 1 nm in diameter are the most abundant ones for the batches used, this leads to the presence, on average, of one molecule of **1** for every 7 nm of SWNT length. This is in overall agreement with the value extrapolated from AFM analysis. The slightly higher value here obtained could arise from the fact that here all the SWNT surface is available for grafting while in the previous case the SWNTs are lying on the SiO_2 surface, which prevents stacking from one direction.

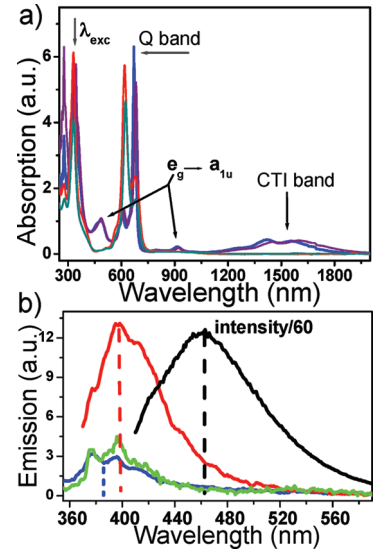

Figure 3. (a) UV/vis/NIR spectra in CH_2Cl_2 for the heteroleptic complex **1** (blue) and the respective homoleptic complex **6** (purple). The spectra of hydrazine hydrate reduced complexes of **1** (red) and **6** (cyan) are also displayed, proving quenching of the intervalence band. (b) Comparison of the emission spectra of the pyrene-containing precursor **8** (black, reduced 60 times), the heteroleptic complex **1** (red), the homoleptic complex **6** (green), and the **1**−SWNT hybrids (blue) (all in CH_2Cl_2).

Spectroscopic Characterization. The characterization by UV−visible/NIR of **1** confirms its electronic structure as well as the neutral charge of the molecule. The UV−visible/NIR spectrum exhibits two B-bands at 328 and 350 nm, a very intense Q-band at 672 nm, and two bands at 480 and 913 nm attributed to the π-levels of the substituted Pc′ ligands (Figure 3a).[30] In the near-IR region, two main bands are observed at 906 nm (with a satellite at 800 nm) and 1300−1800 nm. The high-energy band is related to the radical part and attributed to the $^1e_g(\pi) \rightarrow a_{1u}(\pi)$ transition; the lower-energy band is assigned to an intramolecular charge transfer, whereby these near-IR bands disappear upon reduction of **1** by hydrazine hydrate (1% vv).

The characterization by emission spectroscopy of **1**−SWNT samples (in situ dispersion in CH_2Cl_2, sonicated for 2 h) additionally confirms the supramolecular fixation of **1** to the SWNTs. The emission spectrum of compound **1**, acquired with excitation at $\lambda_{ex} = 340$ nm, shows a series of well-defined peaks in the 350−450 nm region (Figure 3b). These bands correspond to three of the five vibronic bands of pyrene fluorescence and appear at 377, 398, and 412 nm. All these band values are red-shifted by 60 nm with respect to the peak position of pristine pyrene or the pyrene-containing fluorescent moiety **8** (black line), indicating that the electron states of the ligand affect the electronic properties of the pyrene moiety. This is an interesting observation by itself, as it implies that there is an electronic interaction between the pyrene and the Pc moieties, which could be used, in principle, to transmit a magnetic interaction. In any case, this peak is useful to confirm the formation of the **1**−SWNT conjugate, as it is known that $\pi-\pi$-stacking interactions shift and quench the fluorescence of pyrene groups. Comparison of the emission spectra of **1** (Figure 3b, in red) with that of the **1**−SWNT conjugate (Figure 3b, in blue) clearly shows the quenching of the fluorescence of **1**, in agreement with the general tendency of photochemical deactivation of pyrene

(34) Johnson, N. L.; Kotz, S. *Distributions in Statistics. Continuous Multivariate Distributions*; Wiley: New York, 1972.
(35) Brooker, R. J. *Genetics: Analysis and Principles*; McGraw-Hill: New York, 2008.
(36) (a) Bogani, L.; Caneschi, A.; Fedi, M.; Gatteschi, D.; Massi, M.; Novak, M. A.; Pini, M. G.; Rettori, A.; Sessoli, R.; Vindigni, A. *Phys. Rev. Lett.* **2004**, *92*, 207204–8. (b) Bogani, L.; Sessoli, R.; Pini, M. G.; Rettori, A.; Novak, M. A.; Massi, M.; Fedi, M.; Giuntini, L.; Caneschi, A.; Gatteschi, D. *Phys. Rev. B.* **2005**, *72*, 064406/1–064406/10.

derivatives by aggregation with SWNTs. Moreover, we can observe a variation of the relative intensity of the vibronic peaks, which is known to be related to the polarity of the surrounding medium. Therefore, this can be used as an in situ probe of the grafting process onto the SWNT wall, which should change the polarity of the pyrene environment. The vibronic peaks become more pronounced after grafting onto the SWNTs, which is what is expected when passing from a higher-polarity environment to a low-polarity one. The relative intensity of the vibronic bands also changes in accordance with the passage from a more polar to a less polar, aromatic environment.

The emission spectrum of homoleptic terbium(III) complex **6** bearing two Pc ligands with pyrene moieties exhibits quenching of the fluorescence, even without the presence of SWNT. This is consistent with intramolecular $\pi-\pi$-interaction of pyrene chromophores taking place in complex **6**, likely due to syn-directed pyrene groups. The spectrum of **6** strongly resembles that of **1**−SWNT, showing the same vibronic fine structure as indication for a low-polarity environment. Such a strong resemblance is attributed to $\pi-\pi$-stacking interactions, which, while absent in **1** alone, are present in both the **1**−SWNT and **6**. This result highlights the importance of using a heteroleptic pyrene-containing complex **1** for the grafting, so as to monitor the grafting process via optical means. In addition, quenching of the emission of the semiconducting SWNTs was observed in the region of 875−1400 nm; however, this indicator was considered as not being unambiguous, since aggregation of the nanotubes might cause similar quenching.

Magnetic Characterization

The magnetic relaxation has been studied to prove the SMM behavior of the **1**−SWNT conjugates and of complex **1**.

The T dependences of the ac susceptibilities of bulk samples of complex **1** show (Figure 12S, Supporting Information), in agreement with the behavior of homologous nonheteroleptic bis-phtalocyanine $[Pc_2Tb]^0$, the presence of slow relaxation of the magnetization at relatively high temperatures: an out-of-phase signal χ'' appears at 46 K at 1 kHz, and the maximum is shifted when varying the frequency.[8] Below 30 K both χ'' and χ' start increasing again, indicating the presence of non-negligible magnetic interactions among SMMs, in agreement with that observed for the dc susceptibility of undiluted $[Pc_2Tb]$ SMMs.[14] This prevents a reliable extraction of the magnetic energy barrier ΔE from an Arrhenius plot. However, the χ'' plot clearly reveals the presence of a shift in the peak frequency, comparable to that previously reported. The large temperature range over which the χ'' signal is spread is also attributable to intermolecular interactions, which should at least partially disappear in **1**−SWNT conjugates, due to increased inter-SMM distances.

The temperature dependence of the χT product of **1**, as obtained with a SQUID magnetometer, is reported in Figure 12S (Supporting Information). The χT product steadily decreases on lowering the temperature, as expected from the depopulation of the spin levels of the rare-earth. A minimum value of 10.4 emu K/mol is reached at 7 K, and a steady increase is observed below this temperature, indicating the onset of intramolecular magnetic interactions.[14]

The ac susceptibility of the **1**−SWNT conjugates reveals magnetic properties of the conjugate: A χ'' signal appears at even higher T than for bulk **1**, with maxima between 44 K (997.3 Hz) and 27.5 K (1.00 Hz), as shown in Figure 4a. The Arrhenius plot, extracted from the temperatures of the maxima for the frequencies used (Figure 4b) affords $\Delta E = 351$ cm^{-1} with a

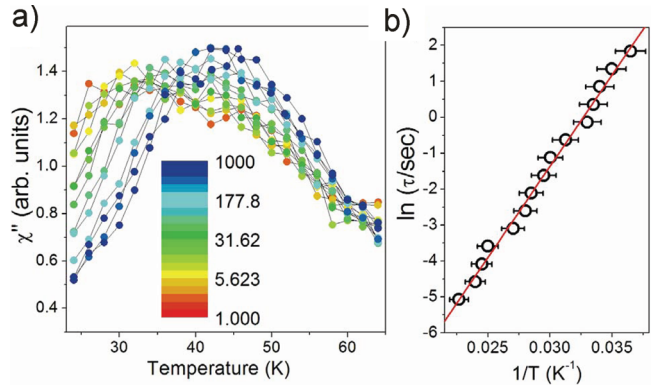

Figure 4. (a) Temperature dependence of the out-of-phase (χ'') components of the ac molar magnetic susceptibility of the **1**−SWNT conjugate and (b) the Arrhenius plot extracted from data in part a proving the SMM behavior.

pre-exponential factor of 6.2×10^{-8} s, in very good agreement with the reported behavior of $[Pc_2Tb]^0$.[8] This confirms the persistence of superparamagnetic behavior in the **1**−SWNT conjugates, showing that the anchored molecules still behave as SMMs. This behavior seems to indicate that the dynamic properties are enhanced, as already reported also for diluted samples of $[Pc_2Tb]^0$ SMMs.[8,14] However, the rather broad peaks in the ac susceptibility, the low signal, and the random orientation of the SMMs in the conjugates do not allow a very accurate comparison. Nevertheless, the energy barrier and the relaxation time of the **1**−SWNT conjugate seems to be increased and lowered, respectively, in comparison to the pure crystalline compound, likely due to the suppression of intermolecular interactions, as similar results have been reported for diluted $[Pc_2Tb]^0$ and $[Pc_2Tb]^{-1}$.[8,14b] Note that this is in strong contrast to recently reported Fe_6-wolframate-based SMMs,[4b] where the relaxation time becomes faster when the respective SMM−SWNT conjugates are produced. This is probably due to the fact that polynuclear transition-metal SMMs are more sensitive to small structural deformations than monocenter rare-earth SMMs.

The persistence of SMM behavior in the conjugates is also evidenced by the opening of a hysteresis cycle at low temperatures (Figure 5), as acquired with a micro-SQUID system.[28] The hysteretic behavior was investigated as a function of temperature and field sweeping rate (see also Figure 13S, Supporting Information). The hysteresis loops of the **1**−SWNT conjugate exhibit increasing hysteresis with increasing field sweep rate at a constant temperature (Figure 5a), increasing hysteresis with decreasing temperature at a constant sweep rate, as expected for the superparamagnet-like properties of a SMM. Close to zero field the cycles present fast relaxation leading to a step at about zero field, which is also the behavior observed for such measurements performed on a powder sample of **1** (Figure 5b). This corresponds to the desired fingerprint of the Tb-based SMM, which shows an increased magnetic relaxation rate close to zero field. It is to be noted that powder measurements of pure SMM complex **1** display a faster relaxation time, close to zero field, than measurements acquired on diluted $[TbPc_2]$ SMMs inserted in a crystalline matrix of diamagnetic $[YPc_2]$ complexes.[9] In the case here presented, **1**−SWNT conjugate, the hysteresis loops are more open at zero field, which would hint to strongly reduced intermolecular interactions. In isolated molecules, tunnelling is forbidden at zero-field because of the Kramer's theorem. As stated before, a system of such kind must have a ground state that is at least doubly degenerate,

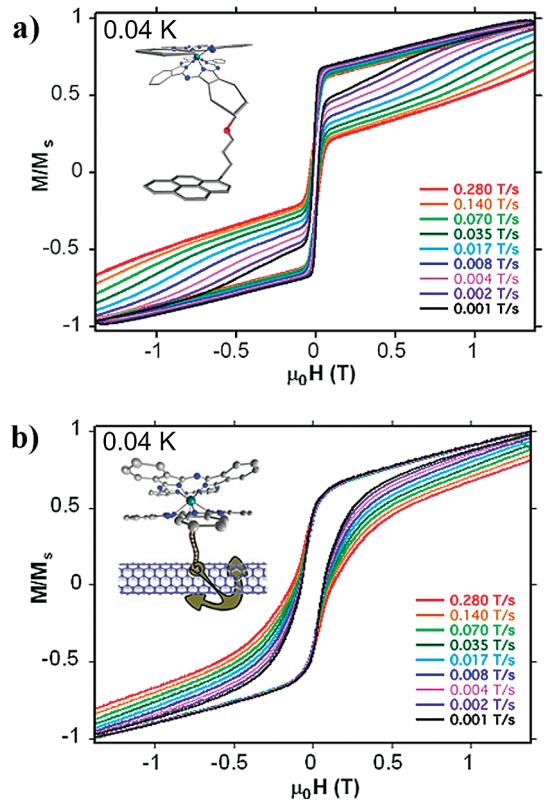

Figure 5. Comparison of the micro-SQUID hysteresis cycles of (a) the **1**−SWNT conjugate and (b) the powder sample of **1** recorded for different scan rates. The hysteresis loops are more open at zero field for the **1**−SWNT conjugate (bottom), a result attributed to strongly reduced intermolecular interactions in the conjugate.

even in the presence of crystal field or spin−orbit interactions or in the presence of strong structural distortions. In the case of terbium, due to hyperfine and nuclear quadrupole interactions, the electronic spin number J is not a good quantum number to calculate parity effects, and we shall consider the sum of nuclear and electronic spin numbers. Terbium practically has only one isotope with 100% abundance and nuclear quantum number $I = 3/2$. The total quantum number is thus a half-integer and no tunnel level splitting is allowed by Kramer's parity theorem. This is reflected in the shape of the cycles of the system, where no neat tunnelling at zero field can be observed. The **1**−SWNT conjugate thus constitutes a perfect example of the desired fingerprint in the magnetic behavior, showing retained and even improved key characteristic feature of the SMMs relaxation in close proximity of SWNTs.

Conclusions

In conclusion, we have synthesized and structurally characterized a new heteroleptic pyrenyl-containing bis-phthalocyanine SMM **1**. The SMM behavior of the bulk complex **1** was proved by ac susceptibility and micro-SQUID investigations. A SMM−SWNT magnetic conjugate was obtained by supramolecular assembly of complex **1** via π-interactions of the pyrene-functionality with highly purified SWNTs (whereby the grafting was qualitatively and quantitatively analyzed using HR-TEM microscopy, emission spectroscopy, AFM imaging, energy-dispersive X-ray, and elemental analysis), yielding an average load of one molecule of **1** per 7−8 nm of SWNT length. Emission spectra before and after the creation of the conjugates indicate that the pyrene groups are actively involved in the grafting, having a different environment in the hybrids than in the crystalline compound or in dichloromethane solutions. This nicely confirms the importance of π-interactions in creating SMM/SWNT hybrids and constitutes an important experimental finding for the future rationalization of interactions between SMM and SWNT, both magnetic and nonmagnetic.

An investigation of the magnetic properties of the SMM−SWNT conjugate was carried out by demonstrating that the SMM behavior is retained and even improved in the hybride systems, in contrast to many d-metal clusters on surfaces.[37] This demonstration is of primary importance for future experiments and also already hints at the possibility of observing different dynamics with respect to crystalline systems.

These results open a chemical route to single rare-earth centers as constituent units for SWNT-based spintronic devices, thus allowing the exploitation of their fingerprint parity effects[7−14] in the quantum tunneling of the magnetization. Moreover, such systems display coherence times longer than those of comparable SMM that have been used to produce SMM−SWNT hybrids,[38] and this could be used for quantum information single-molecule experiments. Eventually, these compounds are very promising candidates for single-molecule magnetic[39] measurements, both when grafted on SWNTs connected to superconducting electrodes, as in the nano-SQUID, and when attached to metallic SWNTs connected to Pd electrodes, which would allow the observation of magneto-Coulomb effects.[18,19] In this context, it is interesting to note that facile bulk scale separation methods have recently become available that yield both pure semiconducting and pure metallic SWNT samples. In the future, we will attempt analogous experiments with correspondingly purified SWNT materials.

Acknowledgment. We thank D. Wang, H. Rössner, and C. Kübel for HR-TEM measurements and A. Burlak for the help in the manuscript preparation. Financial support was provided by Deutsche Forschungsgemeinschaft (DFG), the ERA-NET-Chemistry project "MultiFUN", ANR-PNANO, ANR-06-NANO-27 MolSpintronics and ANR-08-P110_MolNanoSpin, NE-MAGMANET (FP6-NMP3-CT-2005-515767), EC-RTN QuEMolNa (FP6-CT-2003-504880), ERC-08-226558- MolNanoSpin, and the Marie Curie action EIF-041565 MoST.

Supporting Information Available: ^{1}H NMR, UV/vis data, MALDI-TOF MS of compounds **1**, **2**, and **9** and additional microscopic and magnetic characteristics. This material is available free of charge via the Internet at http://pubs.acs.org.

JA906165E

(37) (a) Ehli, C.; Aminur Rahman, G. M.; Jux, N.; Balbinot, D.; Guldi, D. M.; Paolucci, F.; Marcaccio, M.; Paolucci, D.; Melle-Franco, M.; Zerbetto, F.; Campidelli, S.; Prato, M. *J. Am. Chem. Soc.* **2006**, *128*, 11222–11231. (b) Fernando, K. A. S.; Lin, Y.; Wang, W.; Kumar, S.; Zhou, B.; Xie, S.-Y.; Cureton, L. T.; Sun, Y.-P. *J. Am. Chem. Soc.* **2004**, *126*, 10234–10235.
(38) Bertaina, S.; Gambarelli, S.; Tkachuk, A.; Kurkin, I. N.; Malkin, B.; Stepanov, A.; Barbara, B. *Nature Nano.* **2007**, *2*, 39–42.
(39) (a) Ruben, M. *Angew. Chem., Int. Ed.* **2005**, *44*, 1594–1596. (b) Ruben, M.; Lehn, J.-M.; Müller, P. *Chem. Soc. Rev.* **2006**, *35*, 1056–1067. (c) Ruben, M.; Landa, A.; Lörtscher, E.; Riel, H.; Mayor, M.; Görls, H.; Weber, H. B.; Arnold, A.; Evers, F. *Small* **2008**, *4*, 2229–2235.